Non-coding RNA Research 9 (2024) 649–658

Contents lists available at ScienceDirect

Non-coding RNA Research

journal homepage: www.keaipublishing.com/en/journals/non-coding-rna-research

Original Research Article

Long non-coding RNA *LIP* interacts with PARP-1 influencing the efficiency of base excision repair

You Zuo [a,1], Jiaqian He [a,1], Zheng Zhou [a,*], Jingjing Sun [a], Can Ouyang [a], Hui Huang [a], Yajuan Wang [a], Hairong Liu [b], Simon H. Reed [c]

[a] College of Biology, Hunan University, Changsha, 410082, PR China
[b] College of Material Science and Engineering, Hunan University, Changsha, 410082, PR China
[c] Division of Cancer and Genetics, School of Medicine, Cardiff University, Heath Park, Cardiff, CF14 4XN, United Kingdom

ARTICLE INFO

Keywords:
Long non-coding RNAs
LIP
DNA damage response
Base excision repair
Poly (ADP-ribose) polymerase 1

ABSTRACT

In recent years, various long non-coding RNAs (lncRNAs) involved in DNA damage response (DDR) have been identified and studied to deepen our understanding. However, there are rare reports on the association between lncRNAs and base excision repair (BER). Our designed DNA microarray identified dozens of functionally unknown lncRNAs, and their transcription levels significantly increased upon exposure to DNA damage inducers. One of them, named *LIP* (Long noncoding RNA Interacts with PARP-1), exhibited a significant alteration in transcription in response to methyl methanesulfonate (MMS) and temozolomide (TMZ) treatments. *LIP* knockdown or knockout cell lines are sensitive to MMS and TMZ, indicating that *LIP* plays a crucial role in DDR. The loss or insufficiency of *LIP* significantly influences the efficiency of BER in human cells, and it suggests that *LIP* participates in the BER pathway. The interaction between *LIP* and a key factor in BER, poly (ADP-ribose) polymerase 1 (PARP-1), has been confirmed. We identified and characterized *LIP*, a lncRNA, which is involved in DDR, significantly influences BER efficiency, and interacts with the BER key factor PARP-1. This advances our understanding of the connection between lncRNAs and BER, presenting the potential for the discovery of new drug targets.

1. Introduction

The DNA molecule of the genome within cells is constantly susceptible to a variety of lesions, which can be classified based on their origin as either exogenous damage or endogenous damage. These lesions encompass DNA double-strand breaks, nucleotide cross-links, and base mismatches, among others [1]. If DNA damage remains unaddressed, it can have detrimental effects on various cellular activities, such as hindering protein synthesis, impeding genetic material replication, disrupting the cell cycle, and inducing premature cell apoptosis. Ultimately, this can result in genomic instability and lead to cellular oncogenic transformation, paving the way for the development of cancer [2]. Remarkably, cells have evolved the ability to sense DNA damage and propagate signals to initiate DNA repair processes, collectively referred to as the DDR [3]. To counteract each type of lesions, different proteins and ncRNAs are required to maintain the relative integrity and stability of the genome, forming several DNA damage repair pathways. These pathways encompass double-strand break repair, DNA interstrand cross-link repair, nucleotide excision repair, and base excision repair. Through these sophisticated repair mechanisms, cells efficiently uphold the integrity of their genetic material and safeguard against the potential adverse consequences of DNA damage [4].

LncRNAs have been known for many years, and research has revealed that they possess diverse functionalities, playing crucial roles in various biological processes by interacting with macromolecules such as proteins, DNA, or RNA [5]. As investigations continue, it has become evident that the cellular response to DNA damage involves changes in the transcription of many lncRNAs, which, in turn, participate in DDR through different mechanisms [6]. In recent years, the functional mechanisms of several lncRNAs involved in DDR have been elucidated. For instance, the lncRNA *LRIK* interacts with Ku70 and Ku80 to facilitate non-homologous end joining repair [7]. Another lncRNA, *BS-DRL1*, modulates DDR through its interaction with neuronal HMGB1 [8]. Additionally, *lncRNA Meg3* protects endothelial function by regulating

* Corresponding author.
E-mail address: zhouzheng@hnu.edu.cn (Z. Zhou).
[1] Two authors contributed equally.

https://doi.org/10.1016/j.ncrna.2024.03.010
Received 11 December 2023; Received in revised form 7 March 2024; Accepted 20 March 2024
Available online 25 March 2024

DDR [9]. It is interesting that no lncRNAs involved in BER have been identified or studied. Further investigations in this area will undoubtedly deepen our understanding of the intricate roles that lncRNAs play in the complex process of DDR.

BER is a fundamental DNA repair pathway in cells that corrects base mutations resulting from damage caused by oxidative stress, alkylation, deamination, and depurination/depyrimidination [10]. Its significant relevance to cancer development, neurodegenerative disorders, and aging has spurred increasing interest in investigating BER mechanisms and identifying the biomolecules involved in BER and their functional roles [11]. BER is initiated by DNA glycosylases and proceeds through two pathways: short-patch and long-patch repair, each employing distinct proteins for the repair process [12]. Although discovered in 1974, decades of research have only begun to reveal the broader framework of BER, leaving the specific regulatory network and individual regulatory mechanisms of related proteins largely unresolved [13]. Key biomolecules participating in the BER pathway include XRCC1 as a repair scaffold [14,15], DNA polymerase β (pol-β), DNA ligase 1, DNA ligase 3, and PARP-1 [16,17]. Among them, PARP-1 plays a pivotal role in the BER pathway. It can be activated by single-strand break intermediates during BER and subsequently bind to them, recruiting downstream repair factors such as XRCC1 and DNA ligase-3 (Lig-3) for short-patch BER repair of damaged DNA [18]. Throughout the repair process, PARP-1 gradually dissociates from the binding site and further participates in long-patch BER repair [19]. Due to its overexpression in various tumors, PARP-1 serves as a promising molecular target. PARP-1 inhibitors suppress PARP-1 activity, trapping PARP-1 at DNA damage sites, thereby amplifying DNA damage and impeding the DNA repair process. Presently, numerous PARP-1 inhibitors are undergoing clinical trials for several malignancies [20].

In our previous study [7], dozens of unreported ncRNAs have been identified by employing custom microarrays to conduct a screening for lncRNAs that exhibited significant upregulation in cells treated with the DNA damage-inducing agent MMS.

In this study, we identified and characterized a novel lncRNA, *LIP*, which is required for the cellular response to the BER inducer TMZ. Knockdown or knockout *LIP* enhances the cellular sensitivity to TMZ, and the absence of *LIP* significantly impairs BER efficiency. Subsequently, it was revealed that the interaction between *LIP* and the key BER factor PARP-1. Hence, *LIP* is involved in DDR and significantly affects BER efficiency, and this phenomenon may arise from its interaction with the essential BER protein PARP-1.

2. Materials and methods

2.1. Cell culture and transfection

The HeLa (human cervical cancer epithelial cells), 293T (Human renal epithelial cell line), and A549 (non-small cell lung cancer) cell line used in this experiment were cultured in DMEM medium supplemented with 10% (v/v) fetal bovine serum and 1% (v/v) antibiotics, incubated at 37 °C and 5% CO_2 in a CO_2 incubator. The cells used in the experiment were in the exponential growth phase and samples were tested for mycoplasma contamination using PCR before they were used for investigation. Lipofectamine 2000 (Life Technologies) and Vigofect mammalian cell transfection reagent (Vigras Biotechnology (Beijing) Co., Ltd.) were used according to the manufacturer's instructions to transfect HeLa cells with recombinant plasmids or unmodified plasmids to establish *LIP* knockdown and knockout cell lines.

2.2. Cell treatment

After cells were grown to the exponential phase, the culture medium was aspirated, and fresh media containing MMS or TMZ were added. The cells were then incubated in a 37 °C CO_2 incubator for 30 min. After samples were washed with PBS, fresh DMEM medium was added to all samples for further incubation. The total RNA of all samples was isolated by using the Trizol method. Before reverse transcription, DNase I (DNase I, Ambion) was used to digest genomic DNA in the total RNA samples. Then, purified total RNA samples were detected with a UV–vis spectrophotometer to calculate the concentration, and reverse transcription was carried out using a reverse transcription kit. Real-time fluorescence quantitative PCR (qPCR) was performed using UltraSYBR mix (Cwbio) to measure the relative RNA level of tested genes. GAPDH was used as the negative control, and TransScript II Green One-Step RT-qPCR SuperMix (TransGen) was used for RT-qPCR. The primers used for qPCR are listed in the Supplementary Table S1.

2.3. Rapid amplification of cDNA ends (RACE)

5′ RACE and 3′ RACE were conducted using the FirstChoice RLM-RACE Kit (Life Technologies). The primers used in the RACE are listed in Supplementary Table S2. For 5′ RACE, total RNA was treated with calf intestinal alkaline phosphatase and tobacco acid pyrophosphatase, followed by ligation of RNA with 5′ RACE adapter using T4 RNA ligase. Then, the resulting RNA from the above reaction was reverse transcribed using random primers to obtain cDNA, followed by nested PCR. The obtained products were recovered, ligated to the T-vector, transformed, and amplified using blue-white colony selection and sequencing. The experimental procedure of 3′ RACE is similar to 5′ RACE. Reverse transcription is performed based on the known 3′ RACE adapter, followed by experimental steps similar to 5′ RACE.

2.4. Northern blot

Northern blot was performed using the DIG Northern Starter Kit (Roche). DIG-labeled RNA probes were generated by in vitro transcription with T7 RNA polymerase (Roche) and digoxigenin-11-UTP (Roche). Briefly, 30 μg of total RNA was subjected to 1.2% (w/v) agarose gel electrophoresis in MOPS buffer. Subsequently, the RNA was transferred to a positively charged nylon membrane (GE Life Sciences, RPN303B) by capillary blotting and UV cross-linked. Pre-hybridization was carried out at 68 °C in DIG Easy Hyb for 30–60 min, followed by overnight hybridization with DIG-labeled RNA probes at 68 °C. The membrane was washed twice for 5 min at room temperature with 2 × SSC, 0.1% (w/v) SDS, followed by two washes at 68 °C with 0.1 × SSC, 0.1% (w/v) SDS. Detection of the membrane was performed using the CPD-Star detection reagent. The membrane was exposed to standard X-ray film to obtain the image.

2.5. Bioinformatics analysis

Bioinformatics analysis was conducted using probe sequences from the gene chip to determine the genomic location of *LIP* (microarray data relevant to this study is deposited in the NCBI Gene Expression Omnibus under accession number GSE94868 [7]). The CPAT and RNA fold online tools were utilized to predict the coding ability and secondary structure of *LIP*.

2.6. Construction of LIP knockdown vector

The pSliencer 2.0-U6 vector (AM5762, Ambion) was used to knock down *LIP* by siRNA interference. The DNA template of siRNA was prepared by single strand DNA (ssDNA) synthesis one by one. After preparing ssDNA annealing to form double-stranded DNA, the DNA template of siRNA was ligated to the digested vector using T4 DNA ligase (NEB), followed by transformation and colony selection for sequencing.

2.7. Generation of LIP knockout vector

pSpCas9(BB)-2A-Puro (PX459) V2.0 (addgene) was utilized. DNA containing the sgRNA sequence was synthesized in vitro, and after

annealing to form a double-stranded structure, it was ligated to the linearized vector using T4 DNA ligase (NEB). Following transformation, bacterial colonies were selected and prepared vectors were subjected to sequencing.

2.8. Colony formation assay

For each cell line, an appropriate number of cells (500 for *LIP* knockdown HeLa cells; 500 for *LIP* knockout HeLa cells) were seeded in a 6 cm culture dish. After cell attachment, cells were treated with cell culture medium containing 0.2 mM, 0.4 mM, 0.8 mM, and 1.6 mM concentrations of TMZ for 24 h respectively, followed by replacement with fresh DMEM medium. All samples were incubated in a CO_2 incubator. After 10–14 days of cultivation, cell colonies were formed, and colonies of each sample were fixed with methanol. Samples were stained with 0.1% (w/v) crystal violet in 50% (v/v) methanol and were washed 3–5 times with PBS. The colonies of each sample were counted and normalized to the plating efficiencies of untreated samples.

2.9. Alkaline comet assay

Cells were treated with cell culture medium containing 1 mM TMZ for 24 h and then replaced with fresh DMEM medium. Cells of each sample were collected following 0 h, 24 h, and 48 h incubation with normal cell culture medium. Collected cells of each sample were mixed with 1% low-melting agarose and evenly spread on 0.5% normal-melting agarose. After 1-h lysis with lysis buffer at 4 °C, samples were separated with electrophoresis, which was performed at 30 V for 30 min. Subsequently, the samples were stained with 0.02 mg/ml propidium iodide for 30 min. The comets of each cell in all samples were observed and photographed with an inverted fluorescence microscope. The comet images were analyzed using the CASP software.

2.10. RNA pull-down assay

In vitro transcription was performed using biotin RNA labeling mix (Roche) and T7 RNA polymerase (Roche), followed by treatment with RNase-free DNase I (Ambion) and purification with NucleoSpin RNA Clean-up XS (Macherey Nagel) to generate biotinylated *LIP*, antisense *LIP*, and truncated *LIP*. RNA pull-down experiments were conducted following the methods described in the publication [21]. Proteins associated with RNA were separated using 4–12% NuPAGE Bis-Tris gels (Life Technologies) and then subjected to silver staining using the SilverQuest Silver Staining Kit (Life Technologies) for further mass spectrometry analysis.

2.11. Western blot

The experimental steps of WB were strictly conducted according to the protocol outlined in this article [7]. In summary, post-washed cells were lysed using 2 × SDS buffer to collect protein samples, followed by boiling for 5 min. Fifty micrograms of samples and protein markers were separated using 8% SDS-polyacrylamide gel electrophoresis, transferred to a PVDF membrane, and blocked for 1 h. Incubation with primary and secondary antibodies was performed, followed by imaging under the instrument. Quantification of bands was carried out using ImageJ software.

2.12. UV cross-linking RNA immunoprecipitation (UV-RIP)

UV-RIP was performed following the protocol described in the publication [22]. Crosslinking of each sample was carried out using the CL1000 UV Crosslinker (UVP). Antibodies used in the UV-RIP experiment include *anti*-PARP-1 antibody (Chengdu Zhengneng Biotechnology Co., Ltd.) and normal IgG antibody (Chengdu Zhengneng Biotechnology Co., Ltd.). Residual samples were treated with proteinase K (Promega) and RNA was extracted using TRIzol reagent for further analysis. The enriched level of *LIP* was evaluated by RT-qPCR after DNase I treatment.

2.13. Statistics

All statistical analyses and graphical processing were performed using GraphPad Prism 9.0 version (GraphPad Software, San Diego, CA, USA). All data are expressed as mean ± standard deviation (SD) and are obtained from at least three independent samples or experiments ($n \geq 3$). Statistical significance was determined using two-tailed Student's t-test. Significance levels were denoted as × $P < 0.05$, **$P < 0.01$, ***$P < 0.001$.

3. Results

3.1. Characterization of LIP

The transcript of *LIP* is located on human chromosome 18 (54208609–54210240; GRCh38/hg38) (Fig. 1A). Its full length, approximately 2000 bp, was obtained by PCR using primers designed based on the RACE results (Fig. 1B), and this length was consistent with the Northern blotting results (Fig. 1C). Additionally, this identified RNA molecule displayed a very low possibility of protein coding, suggesting it is a lncRNA (Fig. 1D). It predicted that the *LIP* molecule can form stable secondary structures, which include stem-loop structures and bulging bubbles and facilitate interacting with other macromolecules, by employing the RNAfold software (Fig. 1E). Furthermore, according to quantitative RT-PCR analysis of cytoplasmic and nuclear fractions, the results revealed that *LIP* exhibited a distribution pattern similar to *U1*, which mainly located in the nucleus (Fig. 1F).

DNA is predominantly distributed in the cell nucleus, and similarly, *LIP* is primarily located in the cell nucleus, possessing a secondary structure that facilitates binding to macromolecules. Moreover, *LIP* was identified through custom microarray screening as a significantly upregulated lncRNA in cells treated with the DNA damage inducer MMS. All these characterization results collectively suggest that *LIP* has the ability to participate in DDR by binding with certain macromolecules.

3.2. The induced transcription of LIP by DNA damages

Based on previous research, dozens of non-coding unreported RNAs were identified by screening significant transcriptional alteration of lncRNAs in HeLa cells following MMS treatment through custom-designed ncRNA microarrays (specific data can be found in dataset GSE94868 in the NCBI GEO database) [7]. By using RT-qPCR, the significant elevation of *LIP* has been validated following DNA damage induction (identified as Cluster_1836 in the dataset). Following MMS treatment, the transcription level of *LIP* in HeLa cells showed a significant upregulation within 12 h and returned to the baseline level after 48 h (Fig. 2A). With the same treatment, the increased transcription levels of *LIP* in response to DNA damage were observed in 293T and A549 cell lines, suggesting that *LIP* participates in the cellular DDR (Fig. 2B and C). To investigate whether the transcriptional upregulation of *LIP* is related to a specific DNA lesion type, the TMZ was selected to induce DNA lesions, which caused DNA damage primarily eliminated by the BER pathway. According to publications, over 80% of DNA damage induced TMZ consists of N7-methyl guanine and N3-methyl adenine, both repaired through the BER pathway [23,24]. Remarkably, treatment with 1 mM TMZ resulted in a significant upregulation of *LIP* in HeLa cells (Fig. 2C). The transcriptional upregulation of *LIP* was observed in 293T and A549 cell lines after treatment with TMZ at the same concentration (Fig. 2D and E). The three cell lines from different tissues were used to exclude that the MMS and TMZ induced transcriptional elevation is related with tissue specific responses. These results strongly suggest that the significant transcriptional elevation of *LIP* after treatment with DNA damage inducers like TMZ is a part of the cellular DDR in human cells.

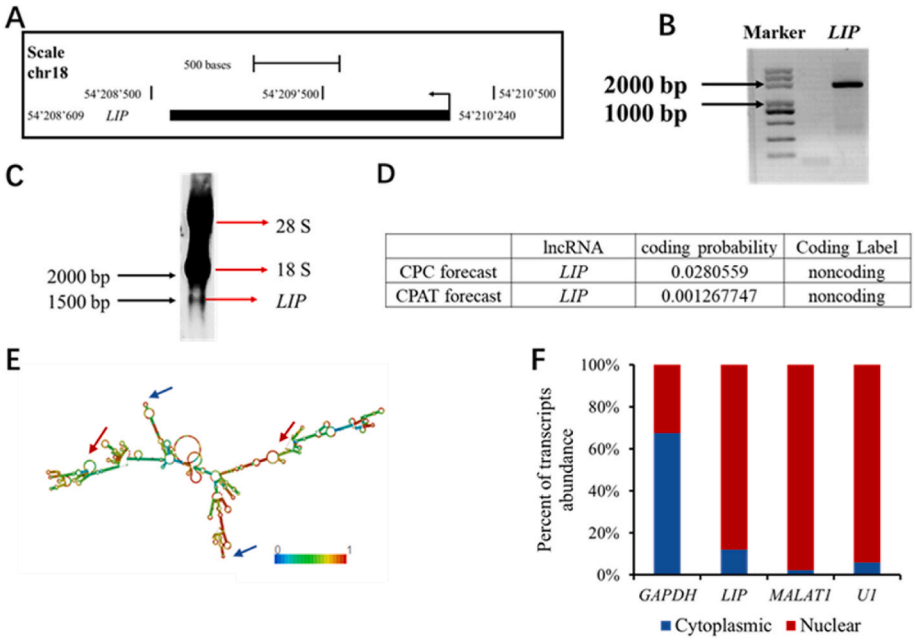

	lncRNA	coding probability	Coding Label
CPC forecast	*LIP*	0.0280559	noncoding
CPAT forecast	*LIP*	0.001267747	noncoding

Fig. 1. Characterization of *LIP*. A. The transcription region of *LIP*. B. Gel image of the full-length amplification of *LIP*. C. Northern blot detecting *LIP* transcripts. D. Prediction of *LIP* coding potential (predicted by CPC and CPAT software) shows that it lacks coding ability. E. Prediction of the secondary structure of *LIP*, with blue arrows representing stem-loop structures, and red arrows representing hairpin structures (predicted by RNAfold software). F. Subcellular distribution of *LIP* examined by RT-qPCR using RNA isolated from cells.

In summary, our research results indicate that the transcription of *LIP* in human cells is upregulated after stimulation with DNA damage agents MMS and TMZ, suggesting its potential association with the BER pathway.

3.3. Knockdown of LIP affects cell survival rate and DNA damage repair efficiency

To further validate the role of DNA damages induced transcription elevation of *LIP* in the cellular DDR, two vectors were prepared to transcribe small hairpin RNAs (shRNAs) targeting different sites of *LIP*, and HeLa cells were infected with prepared vectors to generate a series of *LIP* knockdown cell lines by siRNA interference (Fig. 3A, Supplementary Fig. S1). Cellular survival is affected when damaged DNA cannot be repaired or be repaired with a low efficiency, the colony formation assay was used to assess the cellular survival following tested cells were treated with different DNA damage-inducing reagents, which caused DNA lesions mainly repaired by a specific repair pathway. Compared to the control (shNeg) cell line, two *LIP* knockdown cell lines exhibited significantly increased sensitivity to MMS (Fig. 3B), which is consistent with the transcription of *LIP* induced by MMS treatment (Fig. 2). Similarly, a significantly reduced cellular survival of *LIP* knockdown cell lines was observed after the TMZ treatment compared with the control (shNeg) cell line (Fig. 3C), indicating *LIP* highly likely plays a role in the BER pathway.

To eliminate the possibility of *LIP*'s involvement in other repair pathways, we treated the *LIP* knockdown cell lines with nucleotide excision repair (NER) inducers (UV, 4-Nitroquinoline N-oxide), double-strand break repair inducer (Doxorubicin), and interstrand cross-link repair inducers (Mitomycin, Trioxysalen) and performed colony formation experiments. Interestingly, the survival rate of the LIP knockdown cell lines remained unaffected by the stimulation of these drugs (Supplementary Fig. S2), indicating that *LIP* is specifically involved in the BER pathway.

Since the excision of damaged bases was the essential step during the BER procedure, the alkaline comet assay was utilized to evaluate the efficiency of BER in both control (shNeg) and *LIP* knockdown cell lines following cells were treated with TMZ. At 0 h post-recovery from TMZ treatment, the presence of elongated comet tails indicates the level of DNA damage induced by TMZ in the control group (shNeg) and *LIP* knockdown cells. After 48 h of recovery, the comet tail in *LIP* knockdown cells was still distinct, indicating DNA lesions were incompletely repaired, but the damaged DNA in the shNeg cells was nearly completely repaired (Fig. 3D). The experiment quantitatively analyzed the tail length (Fig. 4E–G) and tail moment (Fig. 4H–J) of both the control (shNeg) and *LIP* knockdown cells. Following TMZ treatment, both control (shNeg) and *LIP* knockdown cells experienced DNA damage, with no statistically significant difference in these tested cells. However, after 24 h and 48 h of recovery, the tail length and tail moment of *LIP* knockdown cells exhibited significantly reduced DNA repair efficiency compared to control (shNeg) cells, suggesting that knockdown of *LIP* reduced the repair efficiency of TMZ-induced DNA damage.

The results indicate that knocking down *LIP* significantly impairs cell BER efficiency, highlighting the crucial role of *LIP* in the BER pathway.

3.4. LIP affects the efficiency of BER

The transcript level of *LIP* significantly decreased using shRNA knockdown technology, without disrupting the genomic DNA sequence of its transcript [25]. Knockdown operates through post-transcriptional regulation but comes with drawbacks, including a high off-target rate, unstable hereditary knockdown efficiency, and incomplete loss of target gene function [26]. To overcome these limitations, we adopted CRISPR-Cas9 technology to introduce mutations in the genomic sequence of *LIP*, disrupting its gene reading frame and resulting in the complete loss of *LIP* function. Using tools available on the internet, four sgRNAs were designed (Fig. 4A), which are capable of knocking out the genomic sequence of *LIP*, and constructed four sgRNA-PX459 recombinant vectors by modifying the PX459 vector with gene engineering methods. To validate the efficiency of the designed sgRNAs, T7E1 enzyme cleavage was used to cut genomic DNA and results demonstrated that they precisely cut and edited the target sites (Supplementary Fig. S3). Subsequently, HeLa cells were co-transfected with two sgRNA-PX459 recombinant vectors with different cleavage sites

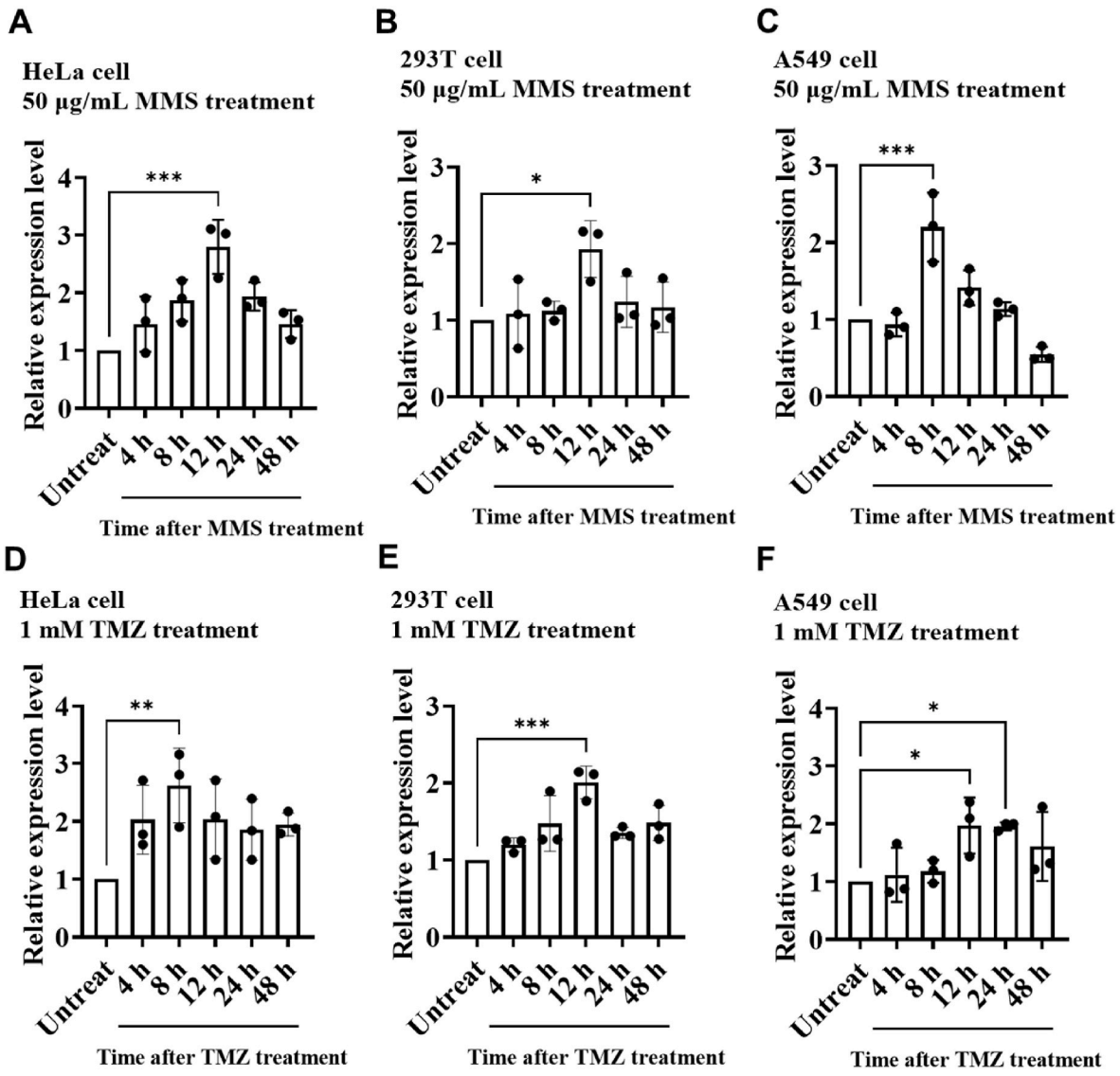

Fig. 2. The induced transcription of LIP by DNA damages. A-C. Significant upregulation of *LIP* transcription in HeLa, 293T, and A549 cells after 50 μg/mL MMS treatment. D-F. Significant upregulation of *LIP* transcription in HeLa, 293T, and A549 cells after 1 mM TMZ treatment. Error bars represent standard deviation (n = 3 independent experiments). *P < 0.05, **P < 0.01, ***P < 0.001, by two-tailed Student's t-test.

respectively to generate a series of *LIP* knockout cell lines. Based on RT-qPCR analysis, two cell lines were selected, which exhibited the highest efficiency of *LIP* knockout (Fig. 4C). Genome sequencing results revealed approximately 11 bp and 800 bp deletions in the *LIP* genomic sequence in these two cell lines (Fig. 4B), accompanied by a substantial number of base mismatches. The two selected cell lines were named KO*LIP*-1 and KO*LIP*-2, respectively, and a negative control cell line (NC) was generated by transfecting HeLa cells with empty PX459 plasmid for further investigation.

After the generation of two *LIP* KO cell lines, the colony formation assay was used to test the TMZ sensitivity of two *LIP* KO cell lines. Following TMZ treatment, it showed the cellular survival of two *LIP* KO cell lines was significantly reduced compared to the control (NC) cell line (Fig. 4D). Results obtained by using the alkaline comet assay displayed that both KO*LIP*-1 and KO*LIP*-2 cells were significantly reduced in efficiency of BER, as significantly more DNA lesions remained after 24 h and 48 h repair compared with the control (NC) cells (Fig. 5A). Quantitative analysis of tail length and tail moment provided evidence that the knockout of *LIP* led to a significant decrease in the efficiency of DNA damage repair following DNA lesions were introduced by TMZ (Fig. 5B–G).

In conclusion, both knockdown and knockout of *LIP* significantly impact cell BER efficiency, confirming the crucial role of *LIP* in the BER pathway induced by TMZ.

3.5. *LIP interacts with PARP-1*

Publications have suggested that lncRNAs interact with macromolecules, like proteins, and participate in pathways possibly by combining with the binding partner [27]. It was predicted by the bioinformatic tool that the loop-stem secondary structure of *LIP* exhibited the capability of interacting with proteins. Thus, we conducted RNA-pulldown combined with mass spectrometry to investigate possible proteins interacting with *LIP*, with which it can influence BER efficiency. Firstly, the RNA pull-down method was applied to identify potential proteins binding to *LIP*, and isolated proteins were separated with PAGE electrophoresis (Fig. 6A). To figure out the right bindings interacting with *LIP*, in vitro-transcribed biotin-labeled *LIP* and full-length antisense RNA were incubated with cell nuclear lysates to capture interacting proteins. The differentially captured protein bands were discovered by gel

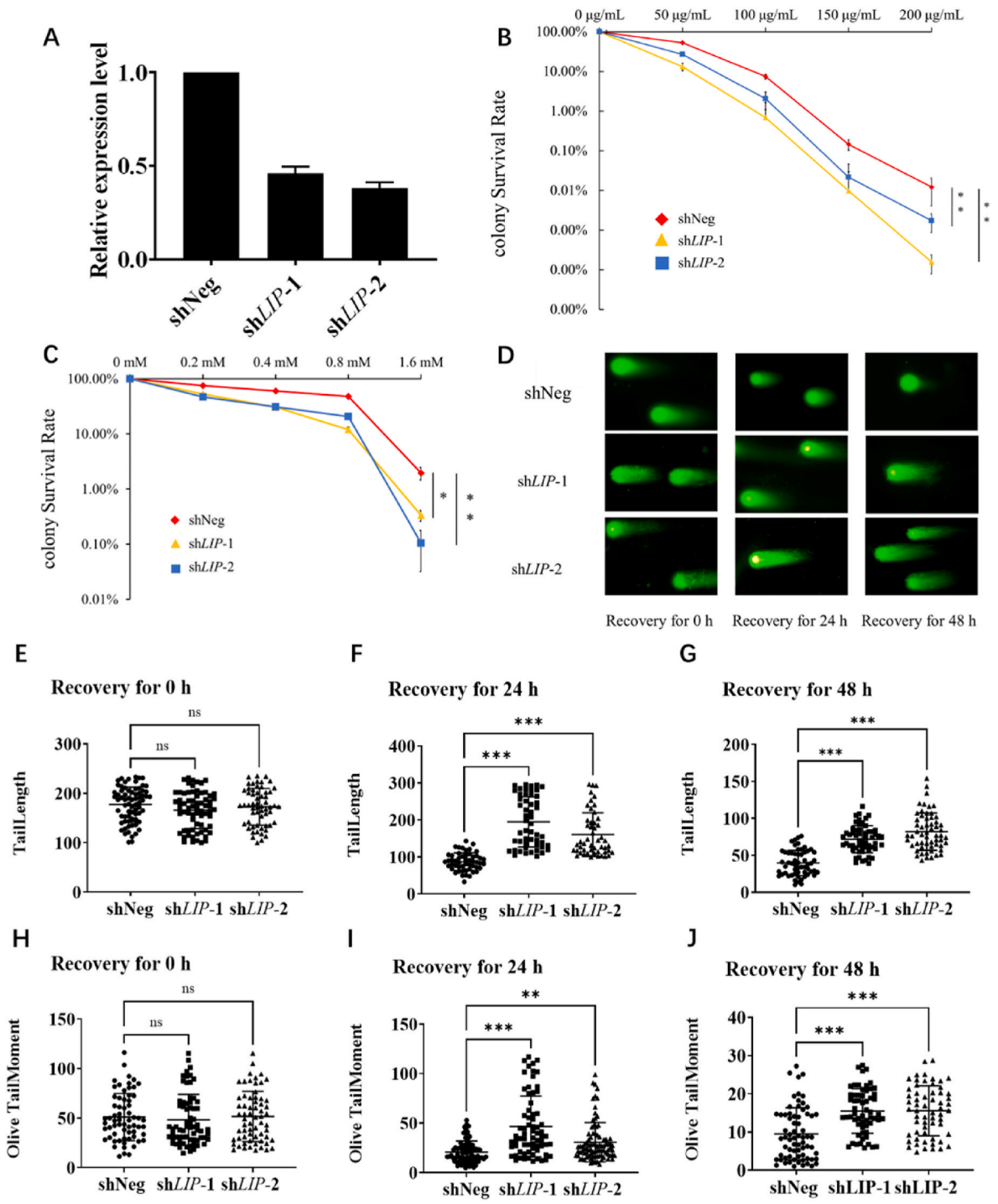

Fig. 3. Knockdown of *LIP* affects cell survival rate and DNA damage repair efficiency. A. RT-qPCR detection of *LIP* transcription levels in *LIP* knockdown cell lines. Colony formation assay. Colony-forming assays suggest that the knockdown of *LIP* inhibits cell survival following treatment with specified concentrations of MMS(B) and TMZ(C). Error bars represent standard deviation (n = 3 independent experiments). *P < 0.05, **P < 0.01, by two-tailed Student's t-test. D. Representative images of comet assays at 0 h, 24 h, and 48 h after 1 mM TMZ treatment in different cell lines. Compared to the control cells, *LIP* knockdown cells show reduced BER repair efficiency (n = 3 independent experiments). *E*-G. Scatter plot showing tail length recovery in different knockdown cell lines after 1 mM TMZ treatment at 0 h, 24 h, and 48 h. h-j. Scatter plot showing tail moment recovery in different knockdown cell lines after 1 mM TMZ treatment at 0 h, 24 h, and 48 h. Ns indicates not significant (summary data from n = 3 independent experiments, with each data point representing >50 cells). *P < 0.05, **P < 0.01, ***P < 0.001, by two-tailed Student's t-test.

electrophoresis combined with silver staining and this binding was analyzed using mass spectrometry. Notably, the mass spectrometry data revealed the presence of a candidate of *LIP*-interacting protein (Fig. 6A the upper panel), PARP-1, known to be involved in the base excision repair pathway (Supplementary Fig. S4). To validate PARP-1 interacting with *LIP*, samples obtained by using the *LIP* pull-down method were analyzed through Western blot immunoblotting assays with *anti*-PARP-1 antibodies (Fig. 6A the lower panel). It is clear that PARP-1 interacts with *LIP* but does not bind to AS-*LIP*, which conforms to the interaction between *LIP* and PARP-1. The interaction between *LIP* and PARP-1

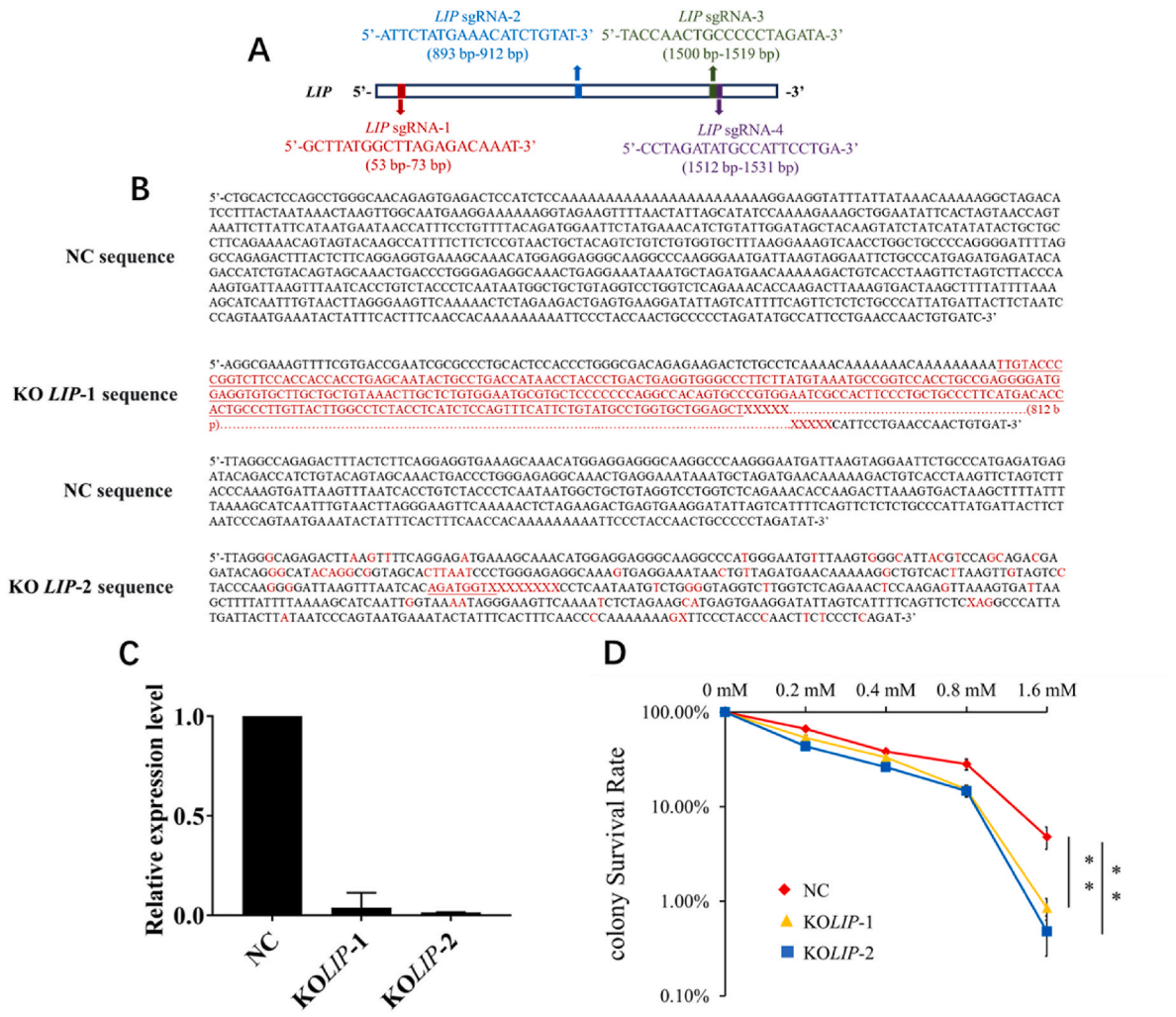

Fig. 4. Knockout of *LIP* affects the cellular survival. Established stable HeLa cell lines with *LIP* knockout using CRISPR/Cas9 technology. A. sgRNA targeting sites and their sequences. B. Genomic sequencing outcomes of the *LIP* knockout cell line, revealing deletions of 812 bp and 11 bp, along with extensive base mismatches. C. RT-qPCR assessment of *LIP* transcript levels in the *LIP* knockout cell line. D. Colony formation experiment, indicating that *LIP* knockout suppressed cell viability after 24 h of TMZ treatment at various concentrations, in comparison to the negative control (NC). Error bars represent standard deviation (n = 3 independent experiments). *P < 0.05, **P < 0.01, by two-tailed Student's t-test.

protein was further confirmed through UV-RIP experiments (Fig. 6B and Supplementary Fig. S5). Following *anti*-PARP-1 antibodies magnetic beads incubated with HeLa cell lysates, macromolecules interacting with PARP-1 were isolated and separated samples were treated with proteinase K to degrade proteins. Then obtained samples were subjected to RT-qPCR analysis, by which to reveal the possible RNA binding partner like *LIP*. Compared to the negative control sample isolated by IgG antibodies magnetic beads, the sample separated by *anti*-PARP-1 magnetic beads showed significant enrichment of *LIP*, with an enrichment fold of approximately 7 times. In summary, our experiments demonstrate that *LIP* significantly influences BER efficiency and interacts with the key BER protein PARP-1 (Fig. 7).

4. Discussion

Although various functions of lncRNAs have been reported, only a few are associated with DNA damage repair. In this study, we identified and characterized a novel lncRNA, *LIP*, primarily localized in the cell nucleus (Fig. 1). Based on its secondary structure, the bioinformatic software predicted its potential interaction with macromolecules. Since DNA damage can induce an upregulation of *LIP* transcription (Fig. 2), firstly whether *LIP* is involved in the cellular DDR was investigated by employing colony-forming assays. Notably, *LIP* knockdown cells are not sensitive to UV, 4-Nitroquinoline N-oxide, Doxorubicin, Mitomycin, and Trioxysalen, but are sensitive to MMS and TMZ (Fig. 3). It emphatically implied that *LIP* participates in the cellular DDR and possibly via the BER pathway.

BER is a critical DNA damage repair pathway that plays a vital role in maintaining genome stability and mutation of genes related to BER contributes to the occurrence and development of various diseases [28]. The subsequent repair can proceed through two pathways: the short patch and the long patch pathways. In the short patch pathway, XRCC1 acts as a scaffold factor to activate polymerase β, which completes DNA synthesis. Then, XRCC1 collaborates with DNA ligase 3 to ligate the synthesized short DNA fragment to the DNA backbone [29]. In the long patch pathway, DNA synthesis requires PCNA, RFC, and polymerases β, δ, and ε, with the involvement of DNA ligase 1 and PCNA for ligation [30,31].

Since during the BER procedure short DNA fragments are generated, the comet assays can be used to monitor the DNA damage repair efficiency. To test whether *LIP* functions in BER, its knockdown cell lines, and the control cell line were first measured by comet assays. The results showed that the knockdown of *LIP* significantly reduced the efficiency of BER (Fig. 3), indicating that *LIP* plays an essential role in this pathway.

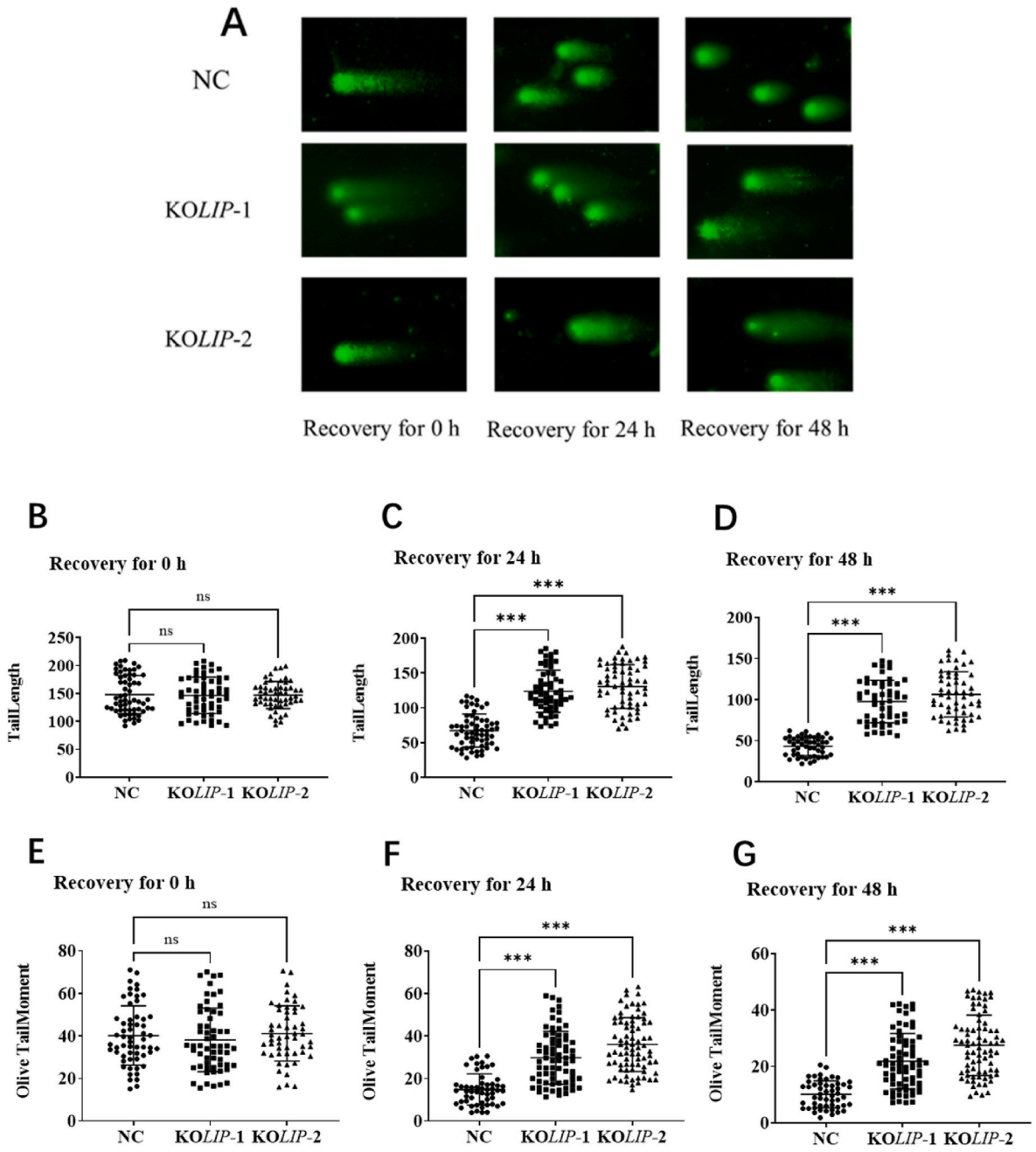

Fig. 5. The comet assay outcomes of the *LIP* knockout cell line. A. Representative comet assay images for various cell lines at 0 h, 24 h, and 48 h after 1 mM TMZ treatment, displaying diminished BER repair efficiency in *LIP* knockout cells compared to control cells (n = 3 independent experiments). B-D. Scatter plots illustrating tail length recovery in different knockout cell lines after 0 h, 24 h, and 48 h of 1 mM TMZ treatment. *E*-G. Scatter plots showing tail moment recovery in different knockout cell lines after 0 h, 24 h, and 48 h of 1 mM TMZ treatment. Ns indicates not significant (displaying summarized data from n = 3 independent experiments, each data point representing cell counts >50). *P < 0.05, **P < 0.01, ***P < 0.001, by two-tailed Student's t-test.

By employing the CRISPR-Cas9 method, *LIP* knockout cell lines, KO*LIP*-1 and KO*LIP*-2 were produced for further confirmation (Fig. 4). In the same way, the DNA damage repair efficiency in KO*LIP*-1 and KO*LIP*-2 cells was significantly declined compared with the control cells (Fig. 5).

As an ADP-ribosyl transferase, PARP-1 plays a critical role in multiple DNA damage repair pathways, but normally it only displays low intrinsic enzymatic activity. The activity of PARP-1 is significantly enhanced following it binds to a single-stranded DNA through its zinc fingers [18,32]. By a combination of the RNA-pulldown method and mass spectrometry, the interaction between *LIP* and PARP-1 has been identified (Fig. 6A), and this interaction has been further confirmed by the immunoprecipitation method with *anti*-PARP-1 antibody (Fig. 6B).

In summary, it has been validated that transcription of *LIP*, a lncRNA, can be induced by DNA damage caused by TMZ. For human cells, knockdown or knockout of *LIP* causes significantly enhanced sensitivity to TMZ. The efficient BER requires *LIP*, since knockdown or knockout of *LIP* results in significantly reduced BER efficiency. The interaction between *LIP* and PARP-1 has been verified, suggesting that *LIP* may influence BER efficiency via its interaction with its interaction with PARP-1 (Fig. 7).

5. Conclusion

The transcriptional induction of *LIP* is a part of the cellular DDR,

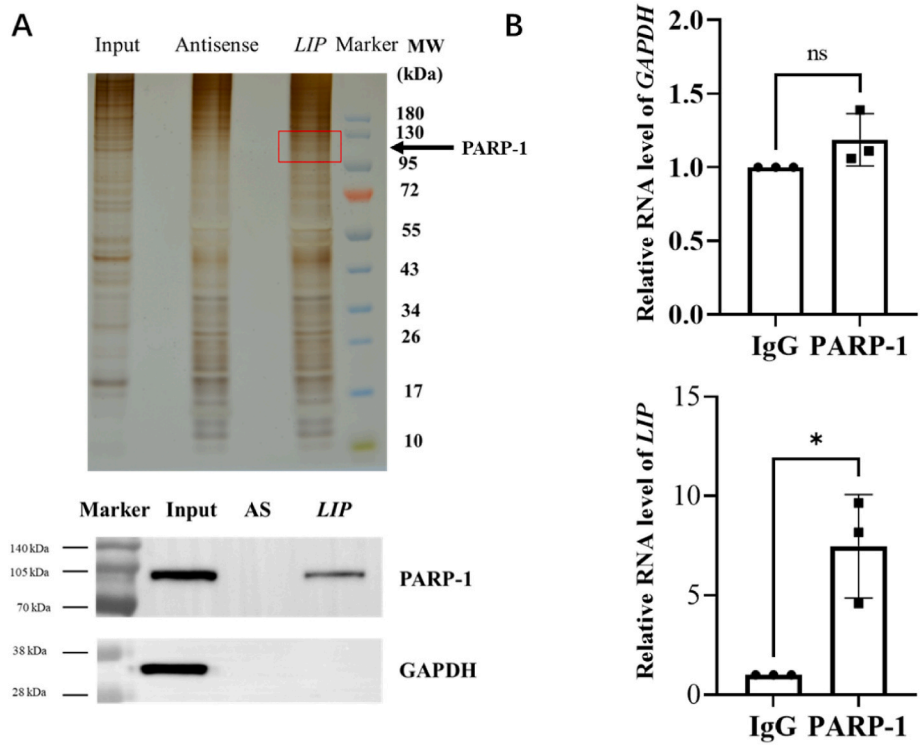

Fig. 6. *LIP* interacts with PARP-1. A. Top, to enrich proteins binding to *LIP*, RNA pull-down assay was performed using biotin-labeled *LIP* incubated with HeLa nuclear extracts. The extracted proteins were subjected to NuPAGE Bis-Tris gel, followed by silver staining and mass spectrometry identification. The red box indicates the differentially present band region, and the arrow indicates the position of PARP-1. Bottom, western blotting analyses following pull-down assays showed the specific interaction between *LIP* and PARP-1. AS indicates the antisense of *LIP*. B. UV cross-linking RIP confirmed the in vivo interaction between *LIP* and PARP-1. Enrichment of PARP-1 for *LIP* in HeLa cells was examined using RT-qPCR. Error bars represent standard deviation (n = 3 independent experiments). *P < 0.05, **P < 0.01, ***P < 0.001, by two-tailed Student's t-test.

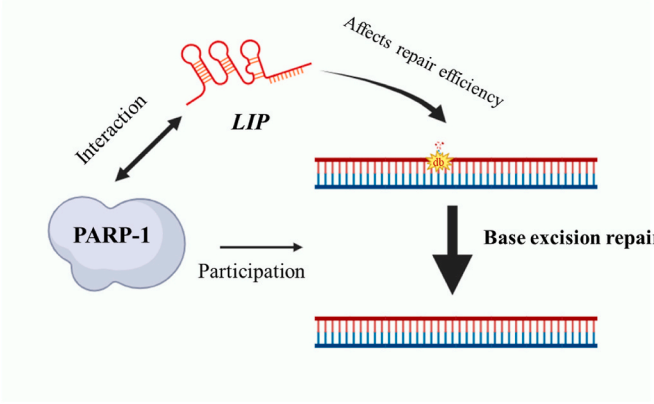

Fig. 7. Model of *LIP* functioning in the BER. *LIP* significantly influences BER efficiency and interacts with the key BER protein PARP-1. db: damage base.

since the absence or insufficient *LIP* causes significantly enhanced TMZ sensitivity to human cells. Knockdown or knockout of *LIP* significantly influences the efficiency of BER, suggesting that sufficient *LIP* is essential for efficient BER. Our data demonstrate that *LIP* selectively interacts with PARP-1, the key BER factor. It is highly likely that *LIP* may participate in BER via interacting with PARP-1 and influencing the efficiency of BER. This study expands the involvement of lncRNA *LIP* in the cellular DDR network and advances our understanding of *LIP* influencing efficient BER.

Funding

The authors sincerely appreciate the support of the National Natural Science Foundation of China [No.31520103905], the Natural Science Foundation of Hunan Province [grant no.2021JJ30095], and the Natural Science Foundation of Changsha City [grant no.kq2014040].

CRediT authorship contribution statement

You Zuo: Writing – original draft, Methodology, Investigation, Formal analysis, Data curation. **Jiaqian He:** Writing – review & editing, Validation, Methodology, Data curation. **Zheng Zhou:** Writing – review & editing, Validation, Supervision, Project administration, Funding acquisition, Conceptualization. **Jingjing Sun:** Software, Resources, Methodology. **Can Ouyang:** Visualization, Data curation. **Hui Huang:** Validation, Methodology. **Yajuan Wang:** Software, Investigation. **Hairong Liu:** Supervision, Project administration, Funding acquisition, Conceptualization. **Simon H. Reed:** Writing – review & editing, Conceptualization.

Declaration of competing interest

The authors declare that they have no known competing financial interests or personal relationships that could have appeared to influence the work reported in this paper.

Acknowledgments

We appreciate the assistance provided by Professor Runsheng Chen and Jianjun Luo (Key Laboratory of RNA Biology, Institute of Biophysics, Chinese Academy of Sciences, Beijing 100101, PR China) in

the experiments and the valuable insights. We thank Dr. Jiyan Zhu and Dr. Dan Wang for their critical suggestions.

Appendix A. Supplementary data

Supplementary data to this article can be found online at https://doi.org/10.1016/j.ncrna.2024.03.010.

References

[1] C.J. Lord, A. Ashworth, The DNA damage response and cancer therapy, Nature 481 (2012) 287–294, https://doi.org/10.1038/nature10760.
[2] N. Hosoya, K. Miyagawa, Targeting DNA damage response in cancer therapy, Cancer Sci. 105 (2014) 370–388, https://doi.org/10.1111/cas.12366.
[3] A. Ciccia, S.J. Elledge, The DNA damage response: making it safe to play with knives, Mol. Cell 40 (2010) 179–204, https://doi.org/10.1016/j.molcel.2010.09.019.
[4] L.Y. Li, Y.D. Guan, X.S. Chen, J.M. Yang, Y. Cheng, DNA repair pathways in cancer therapy and resistance, Front. Pharmacol. 11 (2021) 629266, https://doi.org/10.3389/fphar.2020.629266.
[5] F. Kopp, J.T. Mendell, Functional classification and experimental dissection of long noncoding RNAs, Cell 172 (2018) 393–407, https://doi.org/10.1016/j.cell.2018.01.011.
[6] S.S. Tehrani, A. Karimian, H. Parsian, M. Majidinia, B. Yousefi, Multiple functions of long non-coding RNAs in oxidative stress, DNA damage response and cancer progression, J. Cell. Biochem. 119 (2018) 223–236, https://doi.org/10.1002/jcb.26217.
[7] D. Wang, Z. Zhou, E.R. Wu, C. Ouyang, G.F. Wei, Y.F. Wang, et al., LRIKinteracts with the Ku70-Ku80 heterodimer enhancing the efficiency of NHEJ repair, Cell Death Differ. 27 (2020) 3337–3353, https://doi.org/10.1038/s41418-020-0581-5.
[8] M.M. Lou, X.Q. Tang, G.M. Wang, J. He, F. Luo, M.F. Guan, et al., Long noncoding RNA BS-DRL1 modulates the DNA damage response and genome stability by interacting with HMGB1 in neurons, Nat. Commun. 12 (2021) 4075, https://doi.org/10.1038/s41467-021-24236-z.
[9] M. Ali, X. Cheng, M. Moran, S. Haemmig, M.J. Naldrett, S. Alvarez, et al., LncRNA Meg3 protects endothelial function by regulating the DNA damage response, Nucleic Acids Res. 47 (2019) 1505–1522, https://doi.org/10.1093/nar/gky1190.
[10] H.E. Krokan, M. Bjoras, Base excision repair, Cold Spring Harbor Perspect. Biol. 5 (2013) a012583, https://doi.org/10.1101/cshperspect.a012583.
[11] M.J. Edmonds, J.L. Parsons, Regulation of base excision repair proteins by ubiquitylation, Exp. Cell Res. 329 (2014) 132–138, https://doi.org/10.1016/j.yexcr.2014.07.031.
[12] G.L. Dianov, U. Hubscher, Mammalian base excision repair: the forgotten archangel, Nucleic Acids Res. 41 (2013) 3483–3490, https://doi.org/10.1093/nar/gkt076.
[13] A. Chakraborty, N. Tapryal, A. Islam, S. Mitra, T. Hazra, Transcription coupled base excision repair in mammalian cells: so little is known and so much to uncover, DNA Repair 107 (2021) 103204, https://doi.org/10.1016/j.dnarep.2021.103204.
[14] I.I. Dianova, K.M. Sleeth, S.L. Allinson, J.L. Parsons, C. Breslin, K.W. Caldecott, et al., XRCC1-DNA polymerase beta interaction is required for efficient base excision repair, Nucleic Acids Res. 32 (2004) 2550–2555, https://doi.org/10.1093/nar/gkh567.
[15] M.Z. Li, W. Chen, J.J. Cui, Q.Y. Lin, Y.F. Liu, H.X. Zeng, et al., circCIMT silencing promotes cadmium-induced malignant transformation of lung epithelial cells through the DNA base excision repair pathway, Adv. Sci. 10 (2023), https://doi.org/10.1002/advs.202206896.
[16] M.V. Sukhanova, S.N. Khodyreva, N.A. Lebedeva, R. Prasad, S.H. Wilson, O. I. Lavrik, Human base excision repair enzymes apurinic/apyrimidinic endonuclease 1 (APE1), DNA polymerase beta and poly(ADP-ribose) polymerase 1: interplay between strand-displacement DNA synthesis and proofreading exonuclease activity, Nucleic Acids Res. 33 (2005) 1222–1229, https://doi.org/10.1093/nar/gki266.
[17] M. Thomas, J. Li, K. King, A.K. Persaud, E. Duah, Z. Vangundy, et al., PARP1 and POLD2 as prognostic biomarkers for multiple myeloma in autologous stem cell transplant, Haematologica 108 (2023) 2155–2166, https://doi.org/10.3324/haematol.2022.282399.
[18] A. Huber, P. Bai, J.M. de Murcia, G. de Murcia, PARP-1, PARP-2 and ATM in the DNA damage response: functional synergy in mouse development, DNA Repair 3 (2004) 1103–1108, https://doi.org/10.1016/j.dnarep.2004.06.002.
[19] R. Prasad, O.I. Lavrik, S.J. Kim, P. Kedar, X.P. Yang, B.J. Vande Berg, et al., DNA polymerase beta -mediated long patch base excision repair. Poly(ADP-ribose) polymerase-1 stimulates strand displacement DNA synthesis, J. Biol. Chem. 276 (2001) 32411–32414, https://doi.org/10.1074/jbc.C100292200.
[20] C. Thomas, Y.B. Ji, N. Lodhi, E. Kotova, A.D. Pinnola, K. Golovine, et al., Non-NAD-like poly(ADP-ribose) polymerase-1 inhibitors effectively eliminate cancer in vivo, EBioMedicine 13 (2016) 90–98, https://doi.org/10.1016/j.ebiom.2016.10.001.
[21] Z. Xing, A.F. Lin, C.L. Li, K. Liang, S.Y. Wang, Y. Liu, et al., lncRNA directs cooperative epigenetic regulation downstream of chemokine signals, Cell 159 (2014) 1110–1125, https://doi.org/10.1016/j.cell.2014.10.013.
[22] J.F. Xiang, Q.F. Yin, T. Chen, Y. Zhang, X.O. Zhang, Z. Wu, et al., Human colorectal cancer-specific CCAT1-L lncRNA regulates long-range chromatin interactions at the MYC locus, Cell Res. 24 (2014) 513–531, https://doi.org/10.1038/cr.2014.35.
[23] Y.Q. Song, G.D. Li, D. Niu, F. Chen, S.Z. Jing, V.K.W. Wong, et al., A robust luminescent assay for screening alkyladenine DNA glycosylase inhibitors to overcome DNA repair and temozolomide drug resistance, Journal of Pharmaceutical Analysis 13 (2023) 514–522, https://doi.org/10.1016/j.jpha.2023.04.010.
[24] J.B. Tang, D. Svilar, R.N. Trivedi, X.H. Wang, E.M. Goellner, B. Moore, et al., N-methylpurine DNA glycosylase and DNA polymerase beta modulate BER inhibitor potentiation of glioma cells to temozolomide, Neuro Oncol. 13 (2011) 471–486, https://doi.org/10.1093/neuonc/nor011.
[25] H. Han, RNA interference to knock down gene expression, Methods Mol. Biol. 1706 (2018) 293–302, https://doi.org/10.1007/978-1-4939-7471-9_16.
[26] K. Goel, J.E. Ploski, RISC-Y business: limitations of short hairpin RNA-mediated gene silencing in the brain and a discussion of CRISPR/Cas-Based alternatives, Front. Mol. Neurosci. 15 (2022) 914430, https://doi.org/10.3389/fnmol.2022.914430.
[27] J.J. Quinn, H.Y. Chang, Unique features of long non-coding RNA biogenesis and function, Nat. Rev. Genet. 17 (2016) 47–62, https://doi.org/10.1038/nrg.2015.10.
[28] G.J. Grundy, J.L. Parsons, Base excision repair and its implications to cancer therapy, Essays Biochem. 64 (2020) 831–843, https://doi.org/10.1042/ebc20200013.
[29] R.E. London, The structural basis of XRCC1-mediated DNA repair, DNA Repair 30 (2015) 90–103, https://doi.org/10.1016/j.dnarep.2015.02.005.
[30] J.M. Beaver, Y.H. Lai, S.J. Rolle, Y. Liu, Proliferating cell nuclear antigen prevents trinucleotide repeat expansions by promoting repeat deletion and hairpin removal, DNA Repair 48 (2016) 17–29, https://doi.org/10.1016/j.dnarep.2016.10.006.
[31] K. Blair, M. Tehseen, V.S. Raducanu, T. Shahid, C. Lancey, F. Rashid, et al., Mechanism of human Lig 1 regulation by PCNA in Okazaki fragment sealing, Nat. Commun. 13 (2022) 7833, https://doi.org/10.1038/s41467-022-35475-z.
[32] A. Sefer, E. Kallis, T. Eilert, C. Rocker, O. Kolesnikova, D. Neuhaus, et al., Structural dynamics of DNA strand break sensing by PARP-1 at a single-molecule level, Nat. Commun. 13 (2022) 6569, https://doi.org/10.1038/s41467-022-34148-1.